https://doi.org/10.5194/egusphere-2026-1989
Preprint. Discussion started: 15 June 2026
© Author(s) 2026. CC BY 4.0 License.

A reference basin based framework for identifying and transferring permafrost hydrological coupling regimes across China

Lei Song[1*], Yanping Li[2*]

[1]College of Hydrology and Water Resources, Hohai University, Nanjing, China

[2]College of Oceanography, Hohai University, Nanjing, China

Corresponding authors.

E-mail addresses:

songlei530@126.com (L. Song),

yanping.li@hhu.edu.cn (Y. Li)

https://doi.org/10.5194/egusphere-2026-1989
Preprint. Discussion started: 15 June 2026
© Author(s) 2026. CC BY 4.0 License.

Abstract

Permafrost degradation is altering runoff generation, subsurface storage, and hydrological connectivity across cold region river basins. Scaling process understanding from well-studied basins to broader permafrost regions remains challenging because the subsurface hydrothermal controls that organize permafrost hydrological coupling are rarely observed at large spatial scales. This study develops a reference basin approach for identifying and transferring permafrost hydrological coupling regimes across China using simplified, broadly available, and process relevant proxy variables. Using the Source Region of the Yellow River as a process constrained reference basin, we construct a two-dimensional process space with two coordinates, dominant control depth DCD and coupling strength C. DCD describes the relative vertical position of hydrological control, while C represents the integrated magnitude of permafrost hydrological linkage. Temporal trajectories in this space are clustered into four coupling regime archetypes. These archetypes are then transferred to broader permafrost regions using a parsimonious proxy set that represents climatic background, topographic setting, and vertically integrated soil thermal organization. To define the applicability boundary, out-of-distribution screening identifies regions where target environmental conditions depart from the reference basin support. The results show coherent regional patterns of coupling regimes across the Qinghai Tibetan Plateau and northeastern permafrost regions, while out-of-distribution areas indicate where the transferred classification is less directly interpretable. The framework provides a bounded and physically interpretable pathway for scaling locally constrained coupling archetypes to broader data sparse regions.

Keywords: permafrost hydrology; hydrological coupling regime; reference basin; DCD–C process space; process-relevant proxy variables; out-of-distribution screening

https://doi.org/10.5194/egusphere-2026-1989
Preprint. Discussion started: 15 June 2026
© Author(s) 2026. CC BY 4.0 License.

1. Introduction

Permafrost in China is widely distributed across the Qinghai Tibetan Plateau (QTP) and the cold regions of northern China. It plays an important role in regulating groundwater storage, surface subsurface connectivity, and basin scale runoff generation and routing processes (Walvoord and Kurylyk, 2016; Cheng and Wu, 2007). Under a warming climate, permafrost degradation continues to alter runoff generation and baseflow recharge patterns in cold region catchments through active layer thickening, ground ice melt, and changes in hydraulic connectivity (Wang et al., 2024; Jiang et al., 2024). However, because ground ice abundance, thermal background, and geomorphic conditions vary greatly among regions, thermokarst disturbance and degradation trigger markedly different hydrological responses in different places (Kokelj et al., 2017; Turetsky et al., 2020). This strong spatial heterogeneity implies that the hydrological effects of permafrost degradation are governed not only by the degree of thaw, but also by region-specific coupling structures, making large-scale assessment and extrapolation intrinsically difficult (Hu et al., 2024).

Existing efforts to assess the hydrological effects of permafrost degradation at broader scales mainly follow three complementary extrapolation pathways. The first is data driven or machine learning based transfer, which has been used to upscale permafrost states, infer deep thermal conditions, or predict hydrological variables from environmental covariates (Pastick et al., 2015; Ran et al., 2021; Huang et al., 2025). Such approaches have greatly improved large scale prediction when sufficient training data and representative predictor coverage are available (Reichstein et al., 2019). The second pathway relies on multi source remote sensing and data assimilation, where observable surface variables such as soil moisture or land surface temperature are dynamically updated using satellite products and filtering schemes (Swenson et al., 2012; Tian et al., 2023). These methods provide valuable constraints on large scale surface and near surface states, while the subsurface process controls that organize permafrost hydrological coupling are less directly observable at broad spatial scales. The third pathway is model parameter regionalization or physically based transfer, in

https://doi.org/10.5194/egusphere-2026-1989
Preprint. Discussion started: 15 June 2026
© Author(s) 2026. CC BY 4.0 License.

which locally calibrated parameters are extended to ungauged basins under environmental or geomorphic similarity assumptions (Gelfan et al., 2017; Jafarov et al., 2018). The interpretability of this pathway is closely linked to the degree of hydrothermal and cryospheric similarity between the source and target domains, which motivates an explicit assessment of transfer applicability. Together, these approaches provide important tools for large scale state estimation, prediction, and model transfer.

Building on these efforts, the present study focuses on how trajectory-based permafrost hydrological coupling archetypes identified in a reference basin can be represented at broader scales using a concise, broadly available, and process relevant proxy set, while retaining a clear basis for physical comparability. This problem is challenging because the process variables that organize subsurface coupling are rarely observable at broad spatial scales (Jafarov et al., 2018; Gao et al., 2021a). Variables such as the vertical distribution of soil ice control, the relative depth of dominant hydrothermal influence, and their temporal evolution are difficult to constrain directly outside well observed basins (Zhou et al., 2014; Tian et al., 2023). As a result, coupling archetypes identified under strong local constraints require a transfer pathway that links them to proxy variables representing climatic background, topographic setting, and vertically integrated soil thermal organization, while also defining where the resulting regional interpretation remains supported by the reference domain. Such a low-dimensional proxy-based design supports bounded transfer of reference basin archetypes in a transparent and operationally tractable way across data sparse permafrost regions.

To address this issue, the source region of the Yellow River (SRYR) is selected as a process-constrained reference basin, where stable and degrading permafrost coexist and strong vertical hydrothermal gradients provide a suitable setting for identifying contrasting coupling behaviors (Wang et al., 2018; Song et al., 2024). We first construct a two-dimensional (2D) DCD-C process space, in which dominant control depth (DCD) describes the relative vertical position of coupling control and coupling strength (C) represents the integrated magnitude of permafrost-hydrological linkage. Temporal

https://doi.org/10.5194/egusphere-2026-1989
Preprint. Discussion started: 15 June 2026
© Author(s) 2026. CC BY 4.0 License.

trajectories in this space are then used to identify coupling regime archetypes in the reference basin. A transfer relationship between environmental conditions and regime types is subsequently established using a parsimonious set of broadly available environmental proxies with clear process relevance, and then applied to the permafrost regions of China. Finally, applicability control is introduced through out-of-distribution (OOD) screening to distinguish mapped classification from physically supported interpretation. The framework therefore provides a unified and low-dimensional pathway for regional comparison, in which trajectory-based coupling archetypes identified in the reference basin are linked to broadly available environmental proxies and accompanied by an explicit applicability boundary.

2. Data and Methods

2.1 Study area and datasets

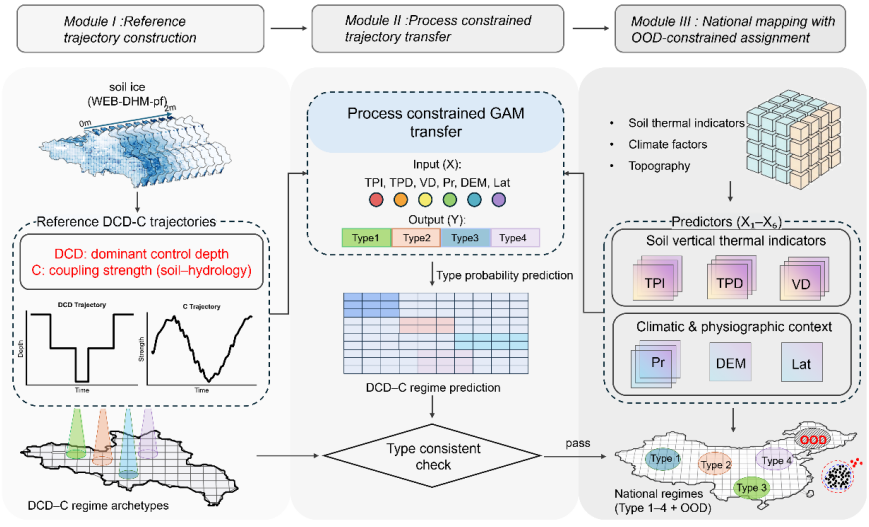

Figure 1. Framework for reference basin based transfer and national mapping of permafrost-hydrological coupling regimes.DCD-C trajectories are first constructed in the reference basin to identify trajectory-based regime archetypes, where DCD denotes dominant control depth and C denotes coupling strength. The archetypes derived from the reference basin are then linked to environmental predictors using a process-constrained generalized additive model (GAM). The

https://doi.org/10.5194/egusphere-2026-1989
Preprint. Discussion started: 15 June 2026
© Author(s) 2026. CC BY 4.0 License.

trained model is subsequently applied to the national domain to predict regime types, and the resulting classification is accompanied by applicability control based on the environmental support represented by the reference basin.

The overall workflow of regime identification, transfer, and applicability control is illustrated in Fig. 1. The SRYR was selected as the reference basin because it contains both stable and degrading permafrost and exhibits pronounced hydrothermal gradients, diverse ground ice conditions, and strong hydrological sensitivity to thaw. The SRYR therefore serves as a process-constrained reference basin for deriving contrasting DCD-C coupling archetypes along a stable-to-degrading permafrost gradient. The broader regional transfer is evaluated through process-relevant environmental proxies and OOD screening, which together define where the reference-basin archetypes remain environmentally supported. The regional transfer domain is limited to the permafrost regions of China, including the major permafrost areas of the QTP and the northeastern cold region. This domain includes both high elevation and high latitude permafrost, spanning strong hydrothermal gradients and contrasting environmental settings. Using this domain as the target transfer range allows us to examine how well the reference-basin prototypes can be expressed under broader regional conditions. It also provides a basis for evaluating the applicability boundary of the proposed framework and the effectiveness of OOD screening.

The datasets used in this study include (1) variables used for process diagnostics in the reference basin and (2) environmental predictors for national transfer. In the reference basin, the soil-state variable used for process diagnostics was soil ice content, derived from previous WEB-DHM-pf (Water and Energy Budget-based Distributed Hydrological Model with permafrost) simulations across the 0-2 m soil profile at 5 km resolution. The hydrological response variable was outlet runoff at the Tangnaihai hydrological station, represented as a monthly time series over 1964-2018 within each analysis window. These variables were used to characterize depth-dependent permafrost-hydrological linkage in the reference basin.

https://doi.org/10.5194/egusphere-2026-1989
Preprint. Discussion started: 15 June 2026
© Author(s) 2026. CC BY 4.0 License.

At the national scale, we used a set of broadly available environmental predictors, including precipitation, latitude, elevation (derived from a digital elevation model, DEM), and three vertically integrated thermal indicators derived from ERA5-Land soil temperature profiles: thermal profile intensity (TPI), thermal penetration depth (TPD), and vertical damping ratio (VD). Raw layer-specific temperatures were not used directly because they describe discrete local states and are less suitable for interregional comparison of vertically organized thermal conditions. Instead, TPI, TPD, and VD were designed as low-dimensional process-relevant proxies that summarize the thermal profile in terms of overall heat input, effective depth of thermal influence, and vertical damping behavior. These indicators are not intended to reconstruct deep process variables directly, but to support regime transfer through comparable representations of vertical thermal organization.

Specifically, TPI characterizes the overall thermal forcing of the soil profile within a given time window and can be interpreted as the depth-integrated positive thermal input. TPD describes the mean depth of thermal influence and can be viewed as the depth-weighted centroid of positive temperature conditions. VD characterizes the attenuation of temperature signals during downward propagation and is defined as the ratio of the temperature amplitude in the deep layer to that in the shallow layer. These three indicators can be expressed as:

$$TPI = \int_0^{z_{max}} T^+(z)\,dz$$

$$TPD = \frac{\int_0^{z_{max}} z\ T^+(z)\,dz}{\int_0^{z_{max}} T^+(z)\,dz}$$

$$VD = \frac{\max(T_{deep}) - \min(T_{deep})}{\max(T_{shallow}) - \min(T_{shallow})}$$

where $T^+(z)$denotes the positive-temperature component of the soil thermal profile that directly contributes to thawing processes, $z$is soil depth, $z_{max}$is the maximum analysis depth, and $T_{deep}$and $T_{shallow}$represent the temperature time series in the deep and shallow soil layers, respectively. Larger VD values indicate weaker attenuation of thermal signals with depth, whereas smaller values indicate stronger damping during

https://doi.org/10.5194/egusphere-2026-1989
Preprint. Discussion started: 15 June 2026
© Author(s) 2026. CC BY 4.0 License.

downward propagation. In practical implementation, these continuous expressions were discretized using the multilayer soil temperature data provided by ERA5-Land.

Taken together, precipitation, latitude, and elevation describe the external climatic and topographic background of permafrost-hydrological coupling, while TPI, TPD, and VD provide complementary information on the vertical thermal structure of the soil profile. These variables jointly constitute the predictor set used for national-scale regime transfer and prediction.

2.2 DCD-C process space and trajectory construction

To characterize the dominant features of permafrost-hydrological coupling in the reference basin, we constructed a 2D process space defined by the dominant control depth (DCD) and the overall coupling strength (C). In this space, DCD represents the vertical location at which coupling is preferentially organized, whereas C represents the integrated magnitude of coupling across the soil profile. Together, these two metrics describe the two basic dimensions of permafrost-hydrological coupling structure, namely vertical position and overall strength, and provide the basis for subsequent regime identification.

We first quantified the coupling strength at each soil depth. Because the response of basin hydrology to permafrost change is not instantaneous, a fixed lag scale was introduced to define coupling consistently across depths. Preliminary lag correlation analyses showed that the main response is concentrated within a short intraseasonal lag range. Based on the monthly runoff time series and preliminary lag-correlation analysis, we used $\tau = 3$ as a representative reference lag and defined the coupling strength at depth z as

$$C(z) = | r(z, \tau = 3) |$$

where $r(z, \tau = 3)$ denotes the correlation coefficient between soil ice content at depth z and runoff response at the fixed lag. The absolute value was used to avoid cancellation caused by differences in correlation direction, thereby providing a stable measure of coupling strength across depths (see Fig. S1 for the sensitivity analysis of τ).

https://doi.org/10.5194/egusphere-2026-1989
Preprint. Discussion started: 15 June 2026
© Author(s) 2026. CC BY 4.0 License.

On this basis, the overall coupling strength C was defined as the cumulative coupling magnitude across the soil profile:

$$C = \sum_{z} C(z)$$

where larger values indicate stronger integrated linkage between permafrost state and hydrological response. The DCD was further defined as the depth-weighted centroid of the vertical coupling-strength distribution:

$$DCD = \frac{\sum_{z} C(z) \cdot z}{\sum_{z} C(z)}$$

where z is the depth of the corresponding layer. DCD is used to represent the vertically dominant depth of coupling strength. It represents the centroid of the overall coupling strength within the soil profile. When coupling is dominated by shallow layers, DCD is small; when deeper control becomes stronger, DCD shifts downward.

Within the reference basin, the depth-specific coupling structure was evaluated using a moving-window scheme over 1964-2018. A 20-year window with a 5-year step was adopted to capture multi-decadal structural evolution while retaining enough samples within each window for stable correlation estimates. This produced eight ordered DCD-C points for each spatial unit, which together formed its temporal trajectory in the process space. These trajectories were then used as input to k-means clustering. Candidate cluster numbers were compared based on physical interpretability. Four clusters were retained because they provided the most balanced partition between structural distinctiveness and physical interpretability; fewer clusters underrepresented key contrasts, whereas more clusters introduced fragmented or physically redundant types. The full diagnostic analysis and comparison of candidate values from k = 2 to k = 8 are provided in Supplementary Figs. S2–S4.

2.3 National transfer and consistency control

After identifying the archetypes of permafrost-hydrological coupling trajectories in the reference basin, a regional transfer framework was developed to extend this type system to the permafrost regions of China and map the spatial distribution of coupling

https://doi.org/10.5194/egusphere-2026-1989
Preprint. Discussion started: 15 June 2026
© Author(s) 2026. CC BY 4.0 License.

regimes. In the national transfer, the trajectory type identified in the reference basin was used as the target variable, while the selected environmental variables were used as predictors.

Using the reference basin as the training domain, precipitation, latitude, elevation, and the vertical thermal indicators TPI, TPD, and VD were taken as the input variables X, and the trajectory type assigned to each spatial unit was used as the target variable Y. A generalized additive model (GAM) was employed to establish the mapping between environmental conditions and coupling types (Hastie and Tibshirani, 1986; Wood, 2017). The model can be expressed as:

$$g[P(Y = k \mid X)] = \beta_{0k} + \sum_{i} f_{ik}(X_i), k = 1,2,\dots,K$$

where Y denotes the trajectory type, X_i represents the environmental predictors, $f_{ik}(\cdot)$ are smooth functions, β_{0k} is the intercept for class k, K is the number of identified types in the reference basin, and $g(\cdot)$ is the link function. For each target grid cell, the model estimated the likelihood of belonging to each type, and the most probable type was assigned.

The derived mapping was then applied to the permafrost regions across China. For each grid cell, the coupling type was predicted based on its environmental conditions, resulting in a spatially continuous classification. All predicted types were expressed under the unified type framework established in the reference basin, allowing the mapped coupling regimes in different regions to be interpreted on a common structural basis.

To account for environmental conditions beyond the support of the training data, an additional applicability screening was introduced. Specifically, environmental support was evaluated relative to the predictor distribution represented by the reference basin, and grid cells falling beyond this support were identified as out-of-distribution (OOD) regions. This labeling was used to indicate where the mapped types were less strongly supported by the reference data, without changing the assigned type itself.

https://doi.org/10.5194/egusphere-2026-1989
Preprint. Discussion started: 15 June 2026
© Author(s) 2026. CC BY 4.0 License.

Through this framework, the coupling archetypes derived from the reference basin were transferred to the national scale under a unified structural reference, while OOD regions explicitly marked where such transfer became less well supported and therefore less directly interpretable.

3. Results

3.1 Regime archetypes and trajectories in the reference basin

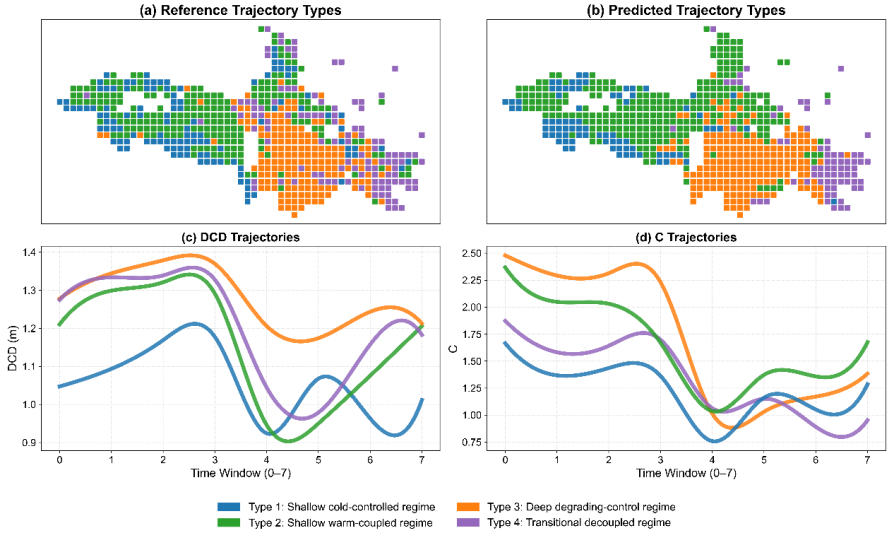

Figure 2. Regime archetypes and their structural characteristics in the reference basin. (a) Spatial distribution of trajectory-based regime archetypes identified from DCD-C trajectories in the reference basin. **(b)** Spatial distribution of predicted regime types in the reference basin. **(c-d)** Temporal evolution of DCD and C for each regime, showing distinct structural trajectory characteristics.

Based on the DCD-C temporal trajectories of individual spatial units within the reference basin, four permafrost-hydrological coupling regimes with stable structural differences were identified. These regimes exhibit clear spatial differentiation (Fig. 2a) and distinct trajectory characteristics in the temporal evolution of dominant control depth (DCD) and coupling strength (C) (Fig. 2c-d). Overall, the differences among regimes are reflected in two main aspects: the vertical position and temporal variation

https://doi.org/10.5194/egusphere-2026-1989
Preprint. Discussion started: 15 June 2026
© Author(s) 2026. CC BY 4.0 License.

of DCD, which indicate the extent to which hydrological processes are controlled by shallow or deep layers, and the magnitude and temporal evolution of C, which reflect changes in the strength of the linkage between hydrothermal state and hydrological response.

Type 1 (shallow cold-controlled regime) is mainly distributed in the cold high-elevation western part of the basin (Fig. 2a). Its DCD remains persistently shallow (approximately 1.0-1.2 m), indicating that hydrological response is primarily controlled by near-surface permafrost processes (Fig. 2c). Meanwhile, its coupling strength remains at a relatively low level, showing only a modest decrease in the middle period and a slight recovery afterward, with limited overall variability (Fig. 2d). This regime is characterized by the coexistence of shallow control and weak coupling, corresponding to a relatively stable hydrological response structure under cold conditions.

Type 2 (shallow warm-coupled regime) is mainly distributed in the central part of the basin (Fig. 2a). Its DCD remains relatively high in the early stage, decreases markedly during the middle period, and then rises again in the later stage (Fig. 2c). Its coupling strength follows a similar pattern, being relatively strong initially, weakening in the middle period, and recovering afterward (Fig. 2d). This trajectory pattern indicates a synchronous adjustment of dominant control depth and coupling strength during the study period, followed by a clear rebound in the later stage. Compared with Type 1, this regime exhibits a stronger hydrothermal-hydrological linkage and greater structural adjustability, reflecting a stage of coupling reorganization followed by renewed strengthening.

Type 3 (deep degrading-control regime) is mainly concentrated in the southeastern part of the basin (Fig. 2a). Its DCD remains the deepest among all four regimes (approximately 1.2-1.4 m), indicating long-term dominance of deeper-layer processes in hydrological response (Fig. 2c). In contrast, its coupling strength is relatively high in the early stage but declines markedly afterward, and although a slight recovery appears in the later stage, it no longer remains the strongest regime (Fig. 2d). This regime

https://doi.org/10.5194/egusphere-2026-1989
Preprint. Discussion started: 15 June 2026
© Author(s) 2026. CC BY 4.0 License.

therefore represents a trajectory of gradually weakening coupling under persistent deep control.

Type 4 (transitional decoupled regime) is mainly distributed in the transition zones between the other regimes (Fig. 2a). Its DCD exhibits a pronounced high-low-high pattern through time, indicating substantial reorganization of the dominant control depth during the study period (Fig. 2c). By contrast, its coupling strength shows a continuous decline and reaches a relatively low level in the later stage (Fig. 2d). This indicates that, although the dominant control layer is being reorganized, the coupling itself does not recover and instead continues to weaken. The regime is therefore characterized by persistent decoupling and can be regarded as a transitional structure between different control modes.

Taken together, the four regimes identified in the reference basin correspond to distinct combinations of control depth and coupling strength in DCD-C space. They can be summarized as a shallow weakly coupled structure, a shallow strongly coupled structure with synchronous adjustment and renewed strengthening, a deep-controlled structure with coupling attenuation, and a transitional structure with persistent decoupling. These regimes provide the structural archetypes for the subsequent regional transfer analysis.

3.2 National distribution of permafrost-hydrological coupling regimes

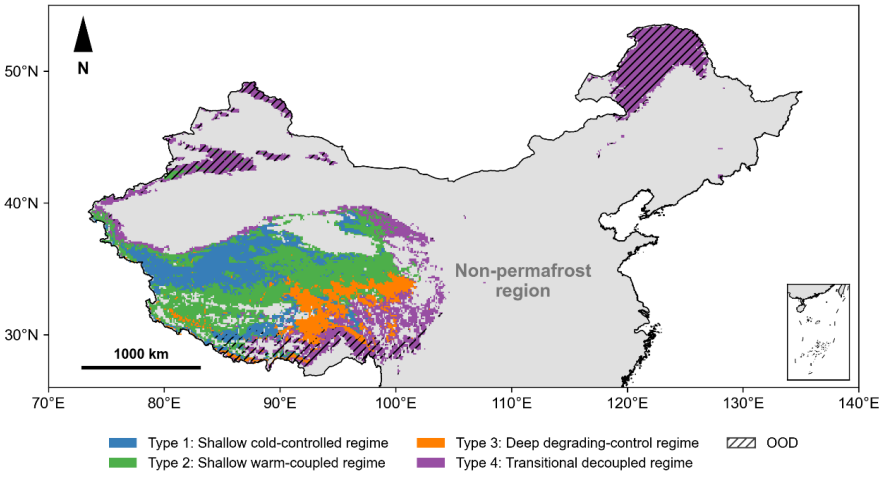

https://doi.org/10.5194/egusphere-2026-1989
Preprint. Discussion started: 15 June 2026
© Author(s) 2026. CC BY 4.0 License.

Figure 3. National distribution of permafrost-hydrological coupling regimes across China. Distinct coupling regimes show strong spatial heterogeneity, particularly across the QTP and other permafrost regions. Areas identified as OOD are marked, indicating regions where environmental conditions extend beyond the support represented by the reference basin.

The transfer relationship between environmental conditions and coupling types was then applied to the permafrost regions across China, resulting in a national map of coupling regime types. Within the reference basin, the transfer reproduced the main spatial contrasts among the original trajectory types, although confusion remained in locally complex transition belts (Fig. 2b). The overall accuracy is 58.15%, with a Kappa coefficient of 0.41, indicating moderate agreement. This level of performance suggests that the framework is better suited to regional structural comparison than to sharp local boundary detection, especially in environments where neighboring archetypes are spatially adjacent and structurally similar.

Furthermore, based on the environmental support represented by the reference basin, an applicability label was assigned to the national prediction results (Fig. 3). The results show that OOD regions are mainly distributed in the high-latitude part of the northeastern permafrost region and in local marginal areas of the QTP. This label is used only to distinguish the applicability range of the results and does not alter the assigned type itself.

On this basis, the national distribution of coupling regimes was further examined (Fig. 3). The results show clear regional differentiation among the identified regimes. Type 1 (shallow cold-controlled regime) is mainly concentrated in the northern part of the Qiangtang Plateau, particularly toward its northwestern margin. Type 2 (shallow warm-coupled regime) is widely distributed across the central interior of the QTP, particularly in the southern Qiangtang Plateau and the Three-River Source region, and is the most widespread regime in the plateau interior. Type 3 (deep degrading-control regime) is mainly concentrated in the southeastern transitional zone of the QTP, forming a relatively continuous southeastward distribution belt. Type 4 (transitional decoupled regime) is mainly distributed along the margins of the QTP and in transition belts where

https://doi.org/10.5194/egusphere-2026-1989
Preprint. Discussion started: 15 June 2026
© Author(s) 2026. CC BY 4.0 License.

different regimes interweave, while also dominating the northeastern permafrost region, where OOD labels are mainly concentrated in the higher-latitude areas.

Overall, the national pattern of permafrost-hydrological coupling regimes shows a gradual spatial transition from west to east and from colder, relatively stable regions toward warmer and wetter degrading regions. The western part is dominated by shallow cold-controlled and shallow warm-coupled regimes, whereas the central and southeastern parts increasingly feature deep degrading-control and transitional decoupled regimes. These results show that the environment-driven transfer framework captures the main spatial differentiation of permafrost-hydrological coupling structures at the regional scale, while also marking areas where applicability is more limited.

3.3 Temporal evolution and transition characteristics of coupling regimes

To further reveal the temporal evolution of permafrost-hydrological coupling structures, we compared the spatial distributions of regime types between the first three time windows (early period) and the last three time windows (late period), and further identified the transition pathways among different types (Fig. 4). Both the early and late periods were classified using the same fixed set of regime archetypes, ensuring direct comparability of the type distributions under a unified reference framework.

From the spatial distributions, the overall regime pattern remains broadly consistent between the early and late periods, but the areal extent and spatial range of different types undergo clear adjustments (Fig. 4a-b). In particular, Type 4 (transitional decoupled regime) expands markedly during the late period, mainly along the margins of the QTP, in the southeastern part of the Plateau, and in some local areas along its northern boundary, while also becoming more extensive in the northeastern permafrost region. Meanwhile, the spatial extent of Type 2 (shallow warm-coupled regime) shows local adjustments in the central and central-western Plateau, and Type 3 (deep degrading-control regime) displays some expansion in the southeastern transitional belt. Overall, the permafrost-hydrological coupling structure exhibits a general shift from relatively strong coupling toward weaker coupling or decoupling, while local

https://doi.org/10.5194/egusphere-2026-1989
Preprint. Discussion started: 15 June 2026
© Author(s) 2026. CC BY 4.0 License.

transitional zones also show structural adjustments from shallow control toward deeper control.

The transition results further reveal the major evolutionary pathways among different coupling structures (Fig. 4c). Among the areas that experience regime changes, the transition from Type 2 to Type 4 accounts for the largest proportion (15.77%). This transition is mainly distributed along the northern margin of the QTP and in the high-latitude northeastern region, reflecting a shift from shallow strongly coupled structures toward decoupled structures in the later period. In addition, the transitions from Type 4 to Type 3 (4.79%) and from Type 2 to Type 3 (2.23%) are mainly concentrated in the southeastern transitional belt of the Plateau, indicating that some areas evolve toward deeper control structures during structural adjustment. The transition from Type 1 to Type 4 (2.91%) is more sparsely distributed along the Plateau margins, suggesting that some shallow cold-controlled structures evolve toward decoupled states under local environmental changes.

At the same time, the extensive gray areas shown in Fig. 4c indicate that a considerable proportion of the region retains the same regime type between the two periods. These stable zones are mainly distributed in the cold western part of the QTP and its continuous permafrost region, indicating relatively strong persistence of coupling structures under cold and comparatively stable environmental conditions.

Overall, the transition patterns indicate a directional tendency toward weaker shallow coupling, stronger structural reorganization, and, in some regions, a downward shift in the dominant control depth in marginal and transitional permafrost zones. Under the adopted archetype framework, these changes represent the dominant shifts in coupling structure at the regional scale.

4. Discussion and conclusions

4.1 Physical implications of coupling types

The four archetypes derived from the DCD-C space should be interpreted as trajectory-based structural prototypes. Although they are identified mathematically,

https://doi.org/10.5194/egusphere-2026-1989
Preprint. Discussion started: 15 June 2026
© Author(s) 2026. CC BY 4.0 License.

their relative positions and temporal behaviors are broadly consistent with contrasting modes of permafrost-hydrological organization reported in previous studies.

Type 1 (Shallow cold-controlled regime) exhibits an extremely shallow control layer and stable weak coupling characteristics, which are highly consistent with the aquiclude effect of stable permafrost (Gruber & Haeberli,2007; Carey & Woo, 2001). Due to the presence of the frozen top layer, deep percolation of precipitation and meltwater is strongly limited, which suppresses infiltration and favors shallow runoff generation while reducing cold season subsurface contribution. This pattern is consistent with shallow flow dominance and limited cold-season subsurface contribution in stable permafrost settings (Gao et al., 2021b; Jiang et al., 2024).

Type 2 (Shallow warm-coupled regime) exhibits strong synergy in thermal depth and nonlinear characteristics of the dipping and rebounding trajectory, which is the most representative coupling structure in the central Tibetan Plateau. This strong coupling essentially reflects the soil reservoir function played by the extensively developed active layer (Cheng and Jin, 2013; Zhao et al., 2019). More importantly, the rebound in both DCD and C may indicate a temporary reorganization followed by renewed shallow coupling. One possible explanation is that changes in near-surface thermal and ecological buffering partially offset further downward heat transfer (Sjöberg et al., 2021), allowing the system to retain relatively strong coupling despite continued disturbance (Shur and Jorgenson, 2007). In this sense, the rebound feature suggests the persistence of relatively organized shallow control under ongoing environmental change.

However, when climate forcing exceeds the buffering threshold of system, degradation will evolve toward two extreme states, Type 3 and Type 4. Type 3 (deep degrading-control regime) is characterized by a stable DCD at the deepest simulated level, accompanied by a marked decline in overall coupling strength (C). This pattern indicates that the dominant control on hydrological response has shifted toward the lower boundary of the active layer, while the synchrony between thermal state and hydrological response becomes weaker. As ground ice near the permafrost table

https://doi.org/10.5194/egusphere-2026-1989
Preprint. Discussion started: 15 June 2026
© Author(s) 2026. CC BY 4.0 License.

continues to melt, deeper thawed soil layers can support stronger subsurface drainage and vertical percolation. In this sense, the Type 3 structure is consistent with the deepening-flow-path pattern reported in degrading permafrost systems (Walvoord and Kurylyk, 2016), and corresponds to a more delayed and subsurface-influenced hydrological response (Wang et al., 2024).

In contrast, Type 4 (transitional decoupled regime) exhibits pronounced oscillation and later rebound in the DCD trajectory, similar to Type 2, but its coupling strength (C) fails to recover synchronously and continues to decrease. This pattern may reflect transient instability during thaw driven restructuring, in which the dominant control layer shifts through time while the overall hydrothermal hydrological linkage weakens. Such behavior is broadly consistent with previous studies reporting increasing heterogeneity, local thaw development, and reorganization of subsurface flow pathways during permafrost degradation (Connon et al., 2014; Connon et al., 2018; Bense et al., 2012). In this sense, Type 4 can be interpreted as a transitional regime between relatively organized shallow control and a more weakly coupled or structurally reorganized subsurface system.

4.2 Temporal evolution features of type transitions

https://doi.org/10.5194/egusphere-2026-1989
Preprint. Discussion started: 15 June 2026
© Author(s) 2026. CC BY 4.0 License.

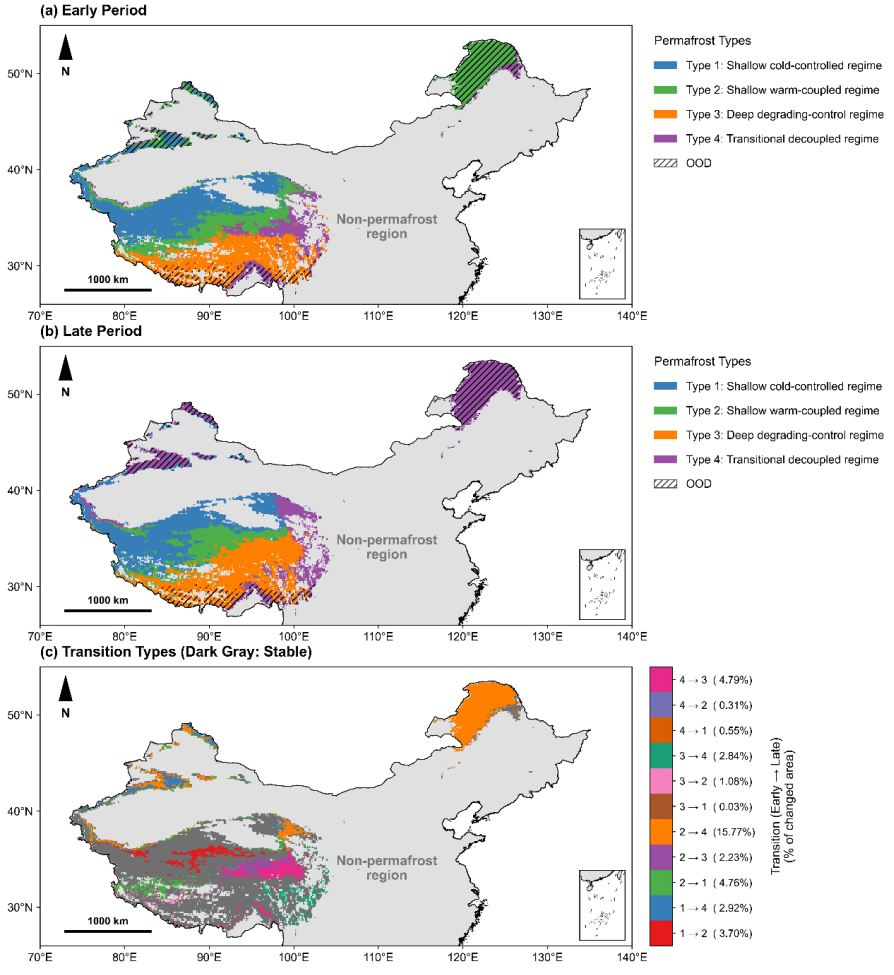

Figure 4. Temporal evolution and transition of permafrost-hydrological coupling regimes. (a) Spatial distribution of regime types during the early period. **(b)** Spatial distribution of regime types during the late period. **(c)** Spatial distribution of regime transitions between the two periods, with stable areas shown in gray.

After clarifying the static physical archetypes, the type shifts that occurred at the regional scale (Figure 4) further reveal the spatial progression gradient and the system dynamics processes of permafrost degradation under climate warming in China. The dominant transition paths identified at the regional scale suggest a broad progression from shallow control toward transitional instability and, in some regions, a downward shift in dominant control depth under continued warming.

https://doi.org/10.5194/egusphere-2026-1989
Preprint. Discussion started: 15 June 2026
© Author(s) 2026. CC BY 4.0 License.

In regions characterized by stable continuous permafrost, such as the Qiangtang Plateau in the western QTP (Zou et al., 2017), the observed transition from Type 1 to Type 2 may indicate an early-stage adjustment of the permafrost-hydrology system under warming conditions. This shift is likely associated with thermal warming of the permafrost table and thickening of the active layer, which together enhance the seasonal storage and release capacity of the shallow soil (Zhao et al., 2010; Gao et al., 2018). As a result, the near surface frozen layer, which previously restricted vertical water exchange, becomes increasingly capable of storing and transmitting water, behaving more like an active supra-permafrost storage layer (Cheng and Jin, 2013). This transition suggests a shift from a system dominated by near-surface runoff toward one with a more pronounced coupling between thermal and hydrological processes.

After accounting for the interpretive uncertainty associated with OOD regions, this study reveals that the most significant evolutionary path in the core area of the QTP (particularly in the Three Rivers Source region) is the transition from Type 4 to Type 3. This evolution represents a shift from a transient decoupling state toward the establishment of a more stable deep-controlled regime. In the early stages of degradation, driven by amplified surface warming (Luo et al., 2016), thawing is not uniform but forms localized thaw zones. This patchy degradation disrupts the shallow hydrological network, but deep vertical pathways remain less developed. Consequently, the system enters a transient Type 4 state, characterized by significant fluctuations in the controlling layer, with decoupling of water-heat relations.

As thaw zones expand, subsurface connectivity may become increasingly established (Ge et al., 2008; Niu et al., 2011), and the system may gradually transition into Type 3. This evolution suggests a shift from a structurally disequilibrated state toward a more stable deep controlled regime. In this sense, the transition from Type 4 to Type 3 is consistent with the observed increase in winter baseflow and the tendency toward stronger subsurface influence in the Three Rivers Source area (Cuo et al., 2015; Wang et al., 2024), as well as reported ecohydrological changes in the region (Jin et al.,

https://doi.org/10.5194/egusphere-2026-1989
Preprint. Discussion started: 15 June 2026
© Author(s) 2026. CC BY 4.0 License.

2022). This transition reflects the permafrost system's adjustment to warming and thawing dynamics.

In contrast, the southeastern margin of the QTP, strongly influenced by the warm and humid monsoon, has become one of the most active regions of permafrost degradation (Cheng and Jin, 2013). The Yarlung Zangbo River Basin (YZRB), although labeled as OOD in the present framework, still shows pronounced structural complexity, with all four types occurring within the basin in the mapped results (Fig. 3). This strong spatial heterogeneity is likely related to the large elevation gradient, complex topography, and intense monsoon-driven hydrothermal forcing in the region (Gao et al., 2021). At broader temporal scales, however, comparison between the early and late periods shows that Type 3 remains dominant in both stages. This suggests that, despite substantial spatial heterogeneity and local structural complexity, the overall coupling structure of the YZRB tends toward deeper control (Yao et al., 2021).

In northeastern China, the large-scale regime pattern shows a clear transition from Type 2 in the early period to Type 4 in the late period, while the national transfer map is also dominated by Type 4 in this region (Fig. 3). This evolution suggests that the northeastern permafrost system has shifted from a shallow warm-coupled structure toward a more weakly coupled and transitional state. Extensive high-latitude areas are simultaneously labeled as OOD, indicating that this high-latitude evolution is represented near the outer boundary of the environmental support covered by the reference basin. Even so, the northeastern pattern forms an important part of the national transition picture by showing that decoupling is not confined to the margins of the QTP, but is also a prominent feature of high-latitude permafrost regions.

4.3 Applicability of the method, regional transfer performance, and limitations

The framework proposed here is designed to transfer trajectory-based coupling archetypes, rather than to reconstruct DCD or C numerically outside the reference basin. In this sense, the environmental predictors serve as process-relevant proxies for expressing locally identified structural types at broader scales. The moderate agreement

https://doi.org/10.5194/egusphere-2026-1989
Preprint. Discussion started: 15 June 2026
© Author(s) 2026. CC BY 4.0 License.

achieved within the reference basin indicates that the framework captures the main regional contrasts among coupling structures, while uncertainty remains greatest in transition zones and environmentally complex areas. Therefore, the regional transfer is focused on macro-scale coupling archetypes, which is more consistent with the level of structural information that can be robustly represented at the regional scale. Although the environmental predictors, including meteorological conditions, terrain, and reconstructed vertical thermal indicators, cannot fully replace real underground ice dynamics, the quantitative evaluation (overall accuracy of 58.15% and Kappa coefficient of 0.41) indicates that this framework can capture the main spatial differentiation of permafrost-hydrological coupling structures in regions lacking deep data, thereby linking process-based archetype identification with proxy-based regional mapping.

Another advantage of this framework is that it explicitly defines the interpretive boundary of regional transfer through OOD control. For example, most of the high-latitude northeastern cold regions were identified as OOD areas. This not only indicates that the model is less well supported in these areas, but also suggests that the framework can identify regions where transfer from the reference basin becomes physically less interpretable. High-latitude permafrost and high-altitude permafrost differ substantially in their dominant energy controls, and the OOD label helps identify where such differences extend beyond the environmental support covered by the reference basin, thereby reducing the risk of unconstrained extrapolation in purely data-based transfer settings.

However, this framework still has certain limitations. First, in structural transition zones with drastic environmental gradients (such as YZRB and other high-altitude regions), macro environmental variables often struggle to precisely distinguish the fragmented features between Type 2 and Type 4, leading to scale effects (scale discrepancies) between large-scale mapping and localized single-point observations. This scale difference may impact the accuracy of regional transfer results. Second, meteorological and soil data (such as ERA5) driving large-scale transfer contain

https://doi.org/10.5194/egusphere-2026-1989
Preprint. Discussion started: 15 June 2026
© Author(s) 2026. CC BY 4.0 License.

inherent uncertainties, and these biases may propagate downstream, affecting the robustness of the proxy relationships. Third, the present framework is based on a single reference basin and may not span the full diversity of process families across China's permafrost regions. Therefore, future studies can further refine the applicability boundary of regional transfer by incorporating higher resolution physical information and enhancing joint cross-validation across multiple basins.

5. Conclusion

This study developed a reference basin based framework for identifying and transferring permafrost-hydrological coupling regimes across China. Using the SRYR as the reference basin, we constructed a DCD-C process space and identified four trajectory-based archetypes that represent contrasting combinations of relative control depth and integrated coupling strength.

The national transfer reveals clear regional differentiation in coupling structures, with shallow-control regimes dominating colder interior regions of the QTP, while deeper-control and transitional decoupled regimes become more common in marginal and environmentally complex zones. The transition analysis further suggests a broad tendency from relatively strong shallow coupling toward weaker or more reorganized structural states under continued warming. OOD screening additionally highlights where national-scale classifications extend beyond the environmental support of the reference basin.

Rather than directly reconstructing local process variables at the national scale, the proposed framework enables the bounded transfer of trajectory-based coupling archetypes derived under stronger local process constraints. In this sense, it provides a feasible pathway for regional comparison of permafrost-hydrological structures in data limited areas. Future work should test the framework across multiple reference basins and incorporate finer-resolution observations to improve both process interpretation and applicability assessment.

https://doi.org/10.5194/egusphere-2026-1989
Preprint. Discussion started: 15 June 2026
© Author(s) 2026. CC BY 4.0 License.

Data availability

ERA5 atmospheric reanalysis is available from the Copernicus Climate Data Store: https://cds.climate.copernicus.eu/datasets/reanalysis-era5-single-levels-monthly-means. Station discharge was taken from the Hydrological Yearbook of the Yellow River Basin (print only volumes; not publicly downloadable). Published by the Ministry of Water Resources of China; years used: 1964-2018.The soil ice simulation outputs used in this study are available from the corresponding author upon reasonable request.

Code availability

The source codes for the analysis of this study are available from the corresponding author upon reasonable request.

Financial support

This study was supported by the Natural Science Foundation of Jiangsu Province under Grant BK20251485, the China Postdoctoral Science Foundation General Program under Grant 2025M770349, and the China Postdoctoral Science Foundation National Postdoctoral Fellowship under Grant GZC20252072.

Author Contributions

S.L. conceived and designed the study, performed the analyses, and wrote the manuscript. Y.L. revised the manuscript for important intellectual content. All authors discussed the results and approved the final version of the manuscript.

Competing Interests

The authors declare that they have no conflict of interest.

https://doi.org/10.5194/egusphere-2026-1989
Preprint. Discussion started: 15 June 2026
© Author(s) 2026. CC BY 4.0 License.

References

Bense, V. F., Kooi, H., Ferguson, G., and Read, T.: Permafrost degradation as a control on hydrogeological regime shifts in a warming climate, J. Geophys. Res.-Earth Surf., 117, F03014, https://doi.org/10.1029/2011JF002143, 2012.

Carey, S. K. and Woo, M.: Spatial variability of hillslope water balance, Wolf Creek basin, subarctic Yukon, Hydrol. Process., 15, 3113-3132, https://doi.org/10.1002/hyp.319, 2001.

Cheng, G. and Jin, H.: Permafrost and groundwater on the Qinghai-Tibet Plateau and in northeast China, Hydrogeol. J., 21, 5-23, https://doi.org/10.1007/s10040-012-0927-2, 2013.

Cheng, G. and Wu, T.: Responses of permafrost to climate change and their environmental significance, Qinghai-Tibet Plateau, J. Geophys. Res.-Earth Surf., 112, F02S03, https://doi.org/10.1029/2006JF000631, 2007.

Connon, R. F., Quinton, W. L., Craig, J. R., and Hayashi, M.: Changing hydrologic connectivity due to permafrost thaw in the lower Liard River valley, NWT, Canada, Hydrol. Process., 28, 4163-4178, https://doi.org/10.1002/hyp.10206, 2014.

Connon, R., Devoie, É., Hayashi, M., Veness, T., and Quinton, W.: The influence of shallow taliks on permafrost thaw and active layer dynamics in subarctic Canada, J. Geophys. Res.-Earth Surf., 123, 281-297, https://doi.org/10.1002/2017JF004469, 2018.

Cuo, L., Zhang, Y., Bohn, T. J., Zhao, L., Li, J., Liu, Q., and Zhou, B.: Frozen soil degradation and its effects on surface hydrology in the northern Tibetan Plateau, J. Geophys. Res.-Atmos., 120, 8276-8298, https://doi.org/10.1002/2015JD023193, 2015.

Gao, B., Yang, D., Qin, Y., Wang, Y., Li, H., Zhang, Y., and Zhang, T.: Change in frozen soils and its effect on regional hydrology, upper Heihe basin, northeastern Qinghai-Tibetan Plateau, The Cryosphere, 12, 657-673, https://doi.org/10.5194/tc-12-657-2018, 2018.

Gao, H., Wang, J., Yang, Y., Pan, X., Ding, Y., and Duan, Z.: Permafrost hydrology of

https://doi.org/10.5194/egusphere-2026-1989
Preprint. Discussion started: 15 June 2026
© Author(s) 2026. CC BY 4.0 License.

the Qinghai-Tibet Plateau: a review of processes and modeling, Front. Earth Sci., 8, 576838, https://doi.org/10.3389/feart.2020.576838, 2021a.

Gao, H., Han, C., Chen, R., Feng, Z., Wang, K., Fenicia, F., and Savenije, H.: Diagnosing the impacts of permafrost on catchment hydrology: field measurements and model experiments in a mountainous catchment in western China, Hydrol. Earth Syst. Sci. Discuss. [preprint], https://doi.org/10.5194/hess-2021-264, 2021b.

Ge, S., Wu, Q. B., Lu, N., Jiang, G., and Ball, L.: Groundwater in the Tibet plateau, western China, Geophys. Res. Lett., 35, L18403, https://doi.org/10.1029/2008GL034809, 2008.

Gelfan, A., Gustafsson, D., Motovilov, Y., Arheimer, B., Kalugin, A., Krylenko, I., and Stepanov, A.: Climate change impact on the water regime of two great Arctic rivers: modeling and uncertainty issues, Clim. Change, 141, 499-515, https://doi.org/10.1007/s10584-016-1710-5, 2017.

Gruber, S. and Haeberli, W.: Permafrost in steep bedrock slopes and its temperature-related destabilization following climate change, J. Geophys. Res.-Earth Surf., 112, F02S18, https://doi.org/10.1029/2006JF000547, 2007.

Hastie, T. and Tibshirani, R.: Generalized additive models, Stat. Sci., 1, 297-310, https://doi.org/10.1214/ss/1177013604, 1986.

Hu, G., Zhao, L., Zou, D., Du, E., Qiao, Y., Sheng, Y., Wu, X., and Wu, T.: Large variability in permafrost degradation over the Northern Hemisphere, Catena, 246, 108440, https://doi.org/10.1016/j.catena.2024.108440, 2024.

Huang, S., Kong, X., Yang, X., Jin, X., Li, S., Yang, L., Zhang, Y., Gao, K., Wang, H., Li, X., He, R., Lü, L., Cheng, G., and Jin, H.: A physics-informed machine learning (PIML) framework for projecting 21st-century permafrost extent in Northeast China, EGUsphere [preprint], https://doi.org/10.5194/egusphere-2025-4544, 2025.

Jafarov, E. E., Coon, E. T., Harp, D. R., Wilson, C. J., Painter, S. L., Atchley, A. L., and Romanovsky, V. E.: Modeling the role of preferential snow accumulation in through talik development and hillslope groundwater flow in a transitional

https://doi.org/10.5194/egusphere-2026-1989
Preprint. Discussion started: 15 June 2026
© Author(s) 2026. CC BY 4.0 License.

permafrost landscape, Environ. Res. Lett., 13, 105006, https://doi.org/10.1088/1748-9326/aadd30, 2018.

Jiang, H., Yi, Y., Yang, K., Zhang, W., and Chen, Y.: Soil freeze thaw dynamics strongly influences runoff regime in a Tibetan permafrost watershed: insights from a process based model, Catena, 243, 108182, https://doi.org/10.1016/j.catena.2024.108182, 2024.

Jin, X., Jin, H., Luo, D., Sheng, Y., Wu, Q., Wu, J., Wang, W., Huang, S., Li, X., Liang, S., Wang, Q., He, R., Serban, R. D., Ma, Q., Gao, S., and Li, Y.: Impacts of permafrost degradation on hydrology and vegetation in the source area of the Yellow River on Northeastern Qinghai-Tibet Plateau, Southwest China, Front. Earth Sci., 10, 845824, https://doi.org/10.3389/feart.2022.845824, 2022.

Kokelj, S. V., Lantz, T. C., Tunnicliffe, J., Segal, R., and Lacelle, D.: Climate driven thaw of permafrost preserved glacial landscapes, northwestern Canada, Geology, 45, 371-374, https://doi.org/10.1130/G38626.1, 2017.

Luo, D., Jin, H., Lü, L., and Zhou, J.: Spatiotemporal changes in extreme ground surface temperatures and the relationship with air temperatures in the Three River Source Regions during 1980-2013, Theor Appl Climatol, 123, 885-897, https://doi.org/10.1007/s00704-015-1543-6, 2016.

Niu, L., Ye, B. S., Li, J., and Sheng, Y.: Effect of permafrost degradation on hydrological processes in typical basins with various permafrost coverage in Western China, Sci. China Earth Sci., 54, 615-624, https://doi.org/10.1007/s11430-010-4073-1, 2011.

Pastick, N. J., Jorgenson, M. T., Wylie, B. K., Nield, S. J., Johnson, K. D., and Finley, A. O.: Distribution of near surface permafrost in Alaska: estimates of present and future conditions, Remote Sens. Environ., 168, 301-315, https://doi.org/10.1016/j.rse.2015.07.019, 2015.

Ran, Y., Li, X., Cheng, G., Nan, Z., Che, J., Sheng, Y., Wu, Q., Jin, H., Luo, D., Tang, Z., and Wu, X.: Mapping the permafrost stability on the Tibetan Plateau for 2005-2015, Sci. China Earth Sci., 64, 62-79, https://doi.org/10.1007/s11430-020-9685-

https://doi.org/10.5194/egusphere-2026-1989
Preprint. Discussion started: 15 June 2026
© Author(s) 2026. CC BY 4.0 License.

3, 2021.

Reichstein, M., Camps Valls, G., Stevens, B., Jung, M., Denzler, J., Carvalhais, N., and Prabhat: Deep learning and process understanding for data driven Earth system science, Nature, 566, 195-204, https://doi.org/10.1038/s41586-019-0912-1, 2019.

Shur, Y. L. and Jorgenson, M. T.: Patterns of permafrost formation and degradation in relation to climate and ecosystems, Permafrost Periglac. Process., 18, 7-19, https://doi.org/10.1002/ppp.582, 2007.

Sjöberg, Y., Jan, A., Painter, S. L., Coon, E. T., Carey, S. K., O'Donnell, J. A., and Schuur, E. A. G.: Permafrost promotes shallow groundwater flow and warmer headwater streams, Water Resour. Res., 57, e2020WR027463, https://doi.org/10.1029/2020WR027463, 2021.

Song, L., Wang, L., Luo, D., Chen, D., and Zhou, J.: Assessing hydrothermal changes in the upper Yellow River Basin amidst permafrost degradation, npj Clim. Atmos. Sci., 7, 57, https://doi.org/10.1038/s41612-024-00607-3, 2024.

Song, L., Wang, L., Zhou, J., Luo, D., and Li, X.: Divergent runoff impacts of permafrost and seasonally frozen ground at a large river basin of Tibetan Plateau during 1960-2019, Environ. Res. Lett., 17, 124038, https://doi.org/10.1088/1748-9326/aca4eb, 2022.

Swenson, S. C., Lawrence, D. M., and Lee, H.: Improved simulation of the terrestrial hydrological cycle in permafrost regions by the Community Land Model, J. Adv. Model. Earth Syst., 4, M08002, https://doi.org/10.1029/2012MS000165, 2012.

Tian, J., Lu, H., Yang, K., Qin, J., Zhao, L., and Jiang, Y.: Improving surface soil moisture estimation through assimilating satellite land surface temperature with a linear SM-LST relationship, IEEE J. Sel. Top. Appl. Earth Obs. Remote Sens., 16, 7777–7790, https://doi.org/10.1109/JSTARS.2023.3305888, 2023.

Turetsky, M. R., Abbott, B. W., Jones, M. C., Anthony, K. W., Olefeldt, D., Schuur, E. A. G., Grosse, G., Kuhry, P., Hugelius, G., Koven, C., Lawrence, D. M., Gibson, C., Sannel, A. B. K., and McGuire, A. D.: Carbon release through abrupt permafrost thaw, Nat. Geosci., 13, 138-143, https://doi.org/10.1038/s41561-019-

https://doi.org/10.5194/egusphere-2026-1989
Preprint. Discussion started: 15 June 2026
© Author(s) 2026. CC BY 4.0 License.

0526-0, 2020.

Walvoord, M. A. and Kurylyk, B. L.: Hydrologic impacts of thawing permafrost-a review, Vadose Zone J., 15, vzj2016.01.0010, https://doi.org/10.2136/vzj2016.01.0010, 2016.

Wang, T., Yang, D., Qin, Y., Wang, Y., Chen, X., Gao, B., and Sen, P.: Historical and future changes of frozen ground in the upper Yellow River Basin, Global Planet. Change, 162, 199-211, https://doi.org/10.1016/j.gloplacha.2018.01.009, 2018.

Wang, Z., Sun, S., Wang, G., and Song, C.: Spatial temporal differentiation of supra and sub permafrost groundwater contributions to river runoff in the Eurasian Arctic and Qinghai Tibet Plateau permafrost regions, Water Resour. Res., 60, e2023WR035913, https://doi.org/10.1029/2023WR035913, 2024.

Wood, S. N.: Generalized Additive Models An Introduction with R, 2nd edn., Chapman and Hall/CRC, Boca Raton, FL, https://doi.org/10.1201/9781315370279, 2017.

Yao, Y., Zheng, C., Andrews, C. B., Scanlon, B. R., Kuang, X., Zeng, Z., Jeong, S.-J., Lancia, M., Wu, Y., and Li, G.: Role of groundwater in sustaining northern Himalayan rivers, Geophys. Res. Lett., 48, e2020GL092354, https://doi.org/10.1029/2020GL092354, 2021.

Zhao, L., Wu, Q., Marchenko, S. S., and Sharkhuu, N.: Thermal state of permafrost and active layer in Central Asia during the international polar year, Permafrost Periglac. Process., 21, 198-207, https://doi.org/10.1002/ppp.688, 2010.

Zhao, L., Hu, G., Zou, D., Wu, X., Ma, L., Sun, Z., Yuan, L., Zhou, H., and Liu, S.: Permafrost changes and its effects on hydrological processes on Qinghai-Tibet Plateau, Bull. Chin. Acad. Sci., 34, 1233 – 1246, https://doi.org/10.16418/j.issn.1000-3045.2019.11.006, 2019.

Zhou, J., Pomeroy, J. W., Zhang, W., Cheng, G., Wang, G., and Chen, C.: Simulating cold regions hydrological processes using a modular model in the west of China, J. Hydrol., 509, 13-24, https://doi.org/10.1016/j.jhydrol.2013.11.013, 2014.

Zou, D., Zhao, L., Sheng, Y., Chen, J., Hu, G., Wu, T., Wu, J., Pang, Q., Ye, B., Cheng, G., and Li, X.: A new map of permafrost distribution on the Tibetan Plateau, The

https://doi.org/10.5194/egusphere-2026-1989
Preprint. Discussion started: 15 June 2026
© Author(s) 2026. CC BY 4.0 License.

752 Cryosphere, 11, 2527-2542, https://doi.org/10.5194/tc-11-2527-2017, 2017.